CHAPTER-2

MATERIALS AND METHOD

The two types of used rechargeable batteries mentioned below have been taken as raw materials to investigate the leaching and recovery of base metals and also the rare earth metals depending upon the case. These batteries are first discharged before dismantling and characterised by chemical analysis, phase identification by XRD (Bruker D8 Discover) and morphology using SEM–EDAX (FEI-Quanta™) studies.

1. Spent lithium ion batteries (LIBs)

2. Spent nickel metal hydride (Ni-MH) batteries

The two batteries are quite different in respect of composition and operational characteristics. One of the best characteristics of a lithium ion battery is its energy-to-weight ratios, producing the same energy as a NiMH battery, but is up to one third lighter than the latter. Due to the benefit of weight, LIBs come in a much wider range of capacities (from 1000 mAh to 4150 mAh), and have neither memory effect nor needed any reconditioning (Wenige et al., 2005). Besides all these operational characteristics the composition and morphology of the two batteries can be distinguished using various techniques.

2.1 Spent lithium ion batteries

Nearly 100 spent LIBs of various make used in laptops, weighing 20 kg were collected from a local service centre as well as from a recycling plant and dismantled were using a manual procedure after discharge.

2.1.1 Dismantling of spent LIBs and characterization of cathode active material

The plastic cases of the batteries were first removed which was followed by removing steel case mechanically. Anode and cathode were uncurled manually, and the cathode active material in the form of powder was separated from aluminum foil by heating the latter at 250-300 ^{o}C for 30 min in a muffle furnace which facilitated the detachment of the cathodic powder. Approximately 1.6 kg cathode active material was recovered from the Al- foils. The powder so obtained was dried and stored for the leaching investigation. The particle size of the cathodic powder was determined by a

laser particle size analyzer (Malvern, UK); size of the particles was found to be < 60 µm and the average size being ~20 µm (Fig. 2.1).
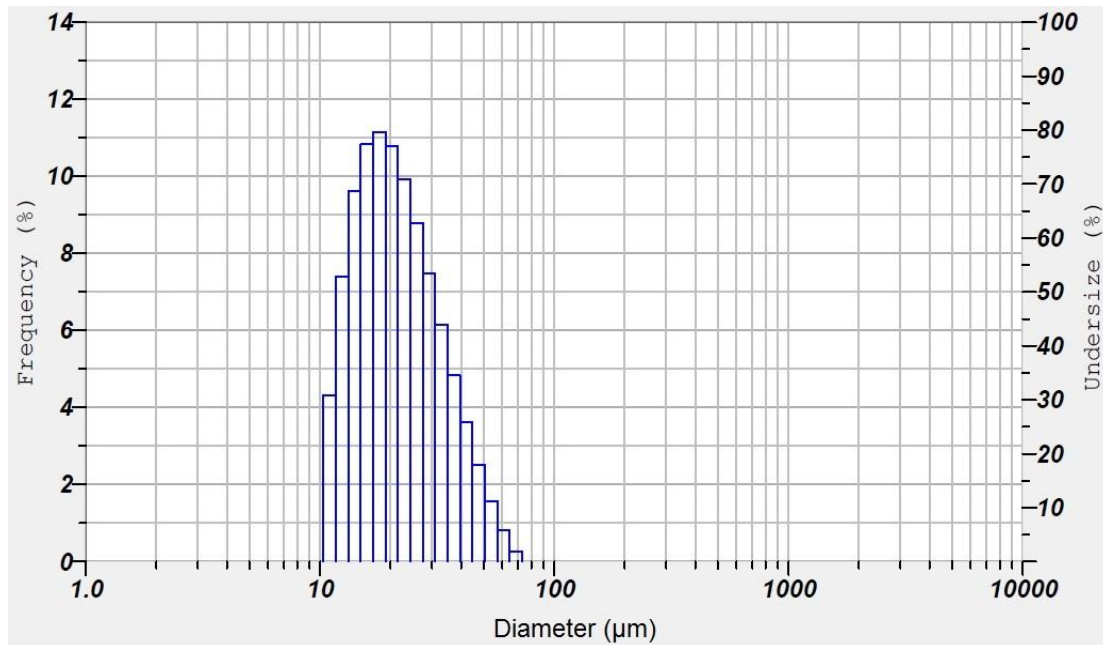

Fig. 2.1. Relative frequency distribution of LIB electrode powder vs diameter (in µm) for particle size analysis

The chemical composition of the cathode active material (Table 2.1) shows the presence of 35.8% Co along with 6.5% Li, 11.6% Mn and 10.6% Ni. Other metals such as copper, aluminium and iron are in smaller amounts. Metals were mostly analysed by Inductively Coupled Plasma - Optical Emission Spectrometer (ICP-OES) (**Varian™, Model: VISTA- MPX)** after digesting the sample in an aqua regia. In some cases Atomic Absorption Spectrometer –AAS **(GBC-980™)** was also used.

Table 2.1: Chemical composition of cathode active material of spent LIBs

Element	Li	Co	Mn	Ni	Cu	Al	Fe
Wt. %	6.5	35.8	11.6	10.06	0.005	0.58	0.06

2.1.2 XRD analysis of cathode active material

The X-ray diffraction analysis of the cathode material (Table 2.2) shows the presence of $LiCoO_2$, $Li_2CoMn_3O_8$ (JCPDS file: 480261) and $(Li_{0.85}Ni_{0.05})(NiO_2)$ as the major constituents (Fig. 2.1). The major constituent of the cathode active material is $LiCoO_2$ in which the average oxidation state of cobalt is +3 (Co^{3+}) while lithium exists in +1 oxidation state (Xiong et al., 2012). Nickel in $(Li_{0.85}Ni_{0.05})(NiO_2)$ is present in +2 state in the layered structure of nickel oxide.The presence of LCM (Li-Co-Mn) based phase viz., $Li_2CoMn_3O_8$, with a distorted spinel structure might have formed as a result of heat generated during the use with a rise in temperature as high as 150 ^{o}C (Julien et al., 2014) and also due to the pre-treatment step (at 250-300 ^{o}C) followed in the present study. In $Li_2CoMn_3O_8$, lithium, cobalt and manganese exist in +1, +2 and +4 oxidation states, respectively. Besides this, lithium-nickel oxide of lower Li-Ni contents, $(Li_{0.69}Ni_{0.01})(NiO_2)$ (JCPDS file: 85-1970) and CoF_4 (JCPDS file 35-1314) were also present as the minor phases as depicted in Fig. 2.2.

Table 2.2: XRD analysis of cathode active material of spent LIBs before processing

Major phase	JCPDS file No.	Minor phase	JCPDS file No.
$LiCoO_2$	77-1370 75-0532	$(Li_{0.69}Ni_{0.01})(NiO_2)$	85-1970
$Li_2CoMn_3O_8$	48-0261	CoF_4	35-1314
$(Li_{0.85}Ni_{0.05})(NiO_2)$	85-1982		

The morphological studies have been carried out by SEM-EDAX techniques. The SEM image (Figs. 2.3 and 2.4) of the cathodic material shows the presence of $LiCoO_2$ particles with irregular morphologies. Also (Fig. 2.3) $LiCoO_2$ particles are present in wider particle size distribution along with large number of secondary particles. The point analysis further confirmed the cobalt distribution all over the materials (point 1, 3 and 4). Nickel and manganese containing phases can be seen as aggregate of particles (point 2). SEM-EDAX analyses with the mapping of constituent elements in cathode material are presented in Fig. 2.4. A look at the elemental mapping shows the lower concentration of cobalt as well as oxygen in the central portion of the

micrograph which is the evidence for the presence of lesser amount of the cobalt containing phase viz., $LiCoO_2$ in this region unlike the metals such as manganese and nickel which are present all around.
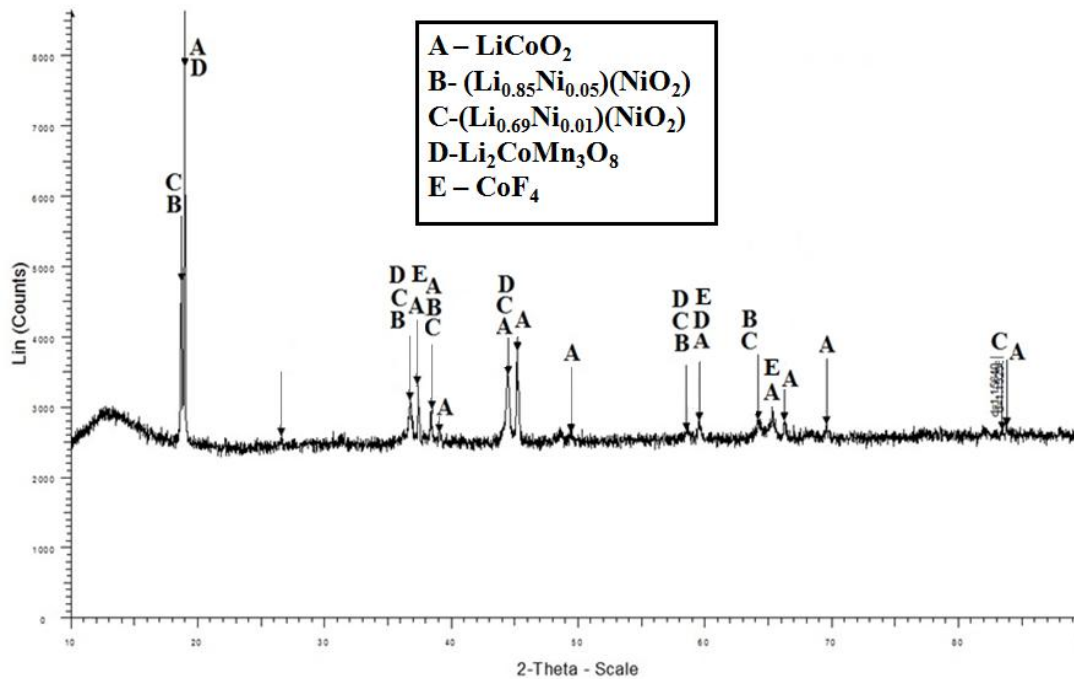

Fig. 2.2: XRD pattern of the cathode active material of spent LIBs along with the identified phases

2.2 Spent nickel metal hydride batteries

The spent Ni-MH batteries (average wt. 57 g each) were collected from the local sources and used in this work. Batteries were dismantled and treated by physical beneficiation method to obtain the electrode material (both anodic and cathodic part). The chemical composition of the electrode powder was determined by ICP-OES (Inductively Coupled Plasma - Optical Emission Spectrometer) after dissolution in the aqua-regia.
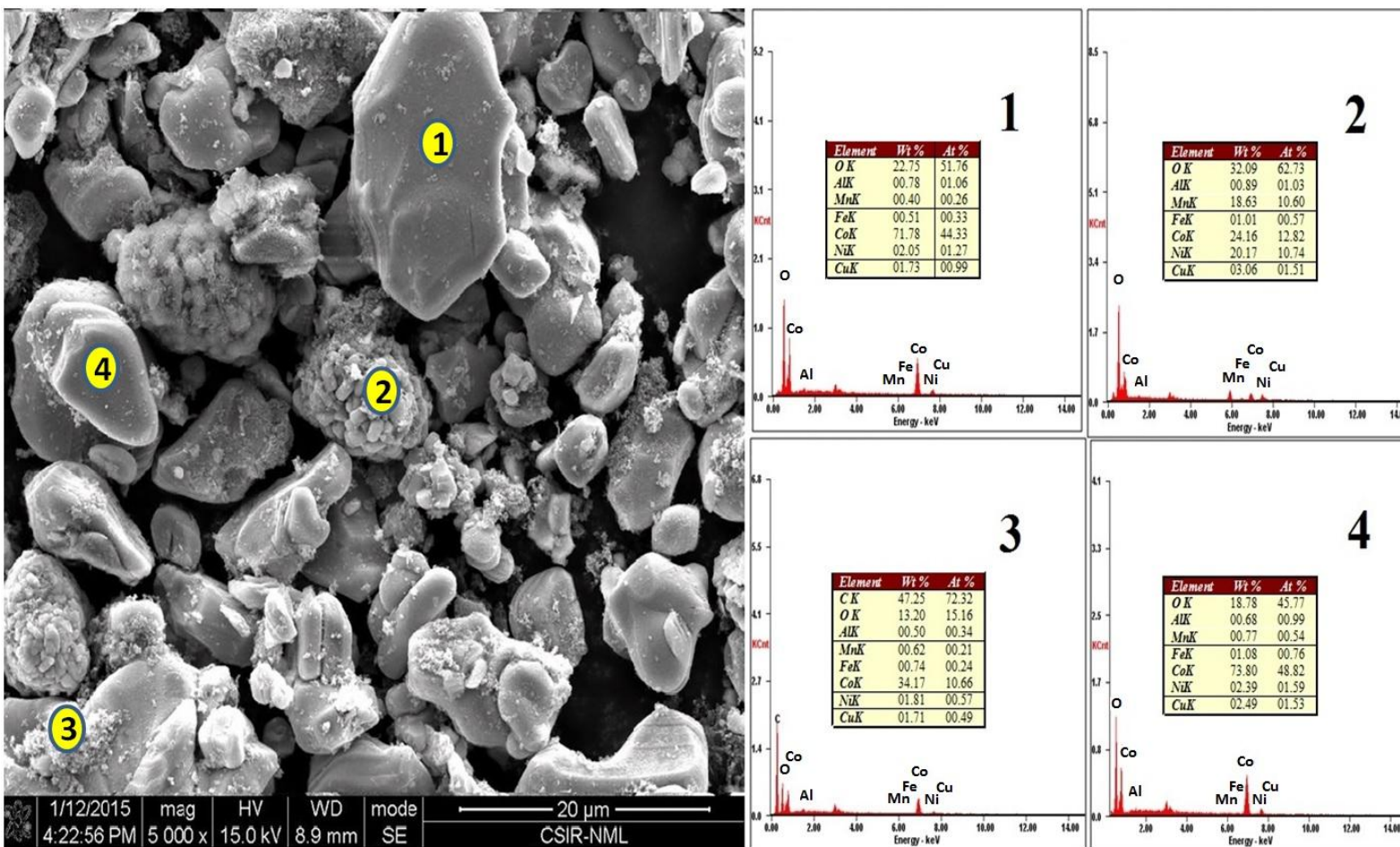
Fig. 2.3: SEM-EDAX with elemental analysis of cathode active material of spent LIBs.
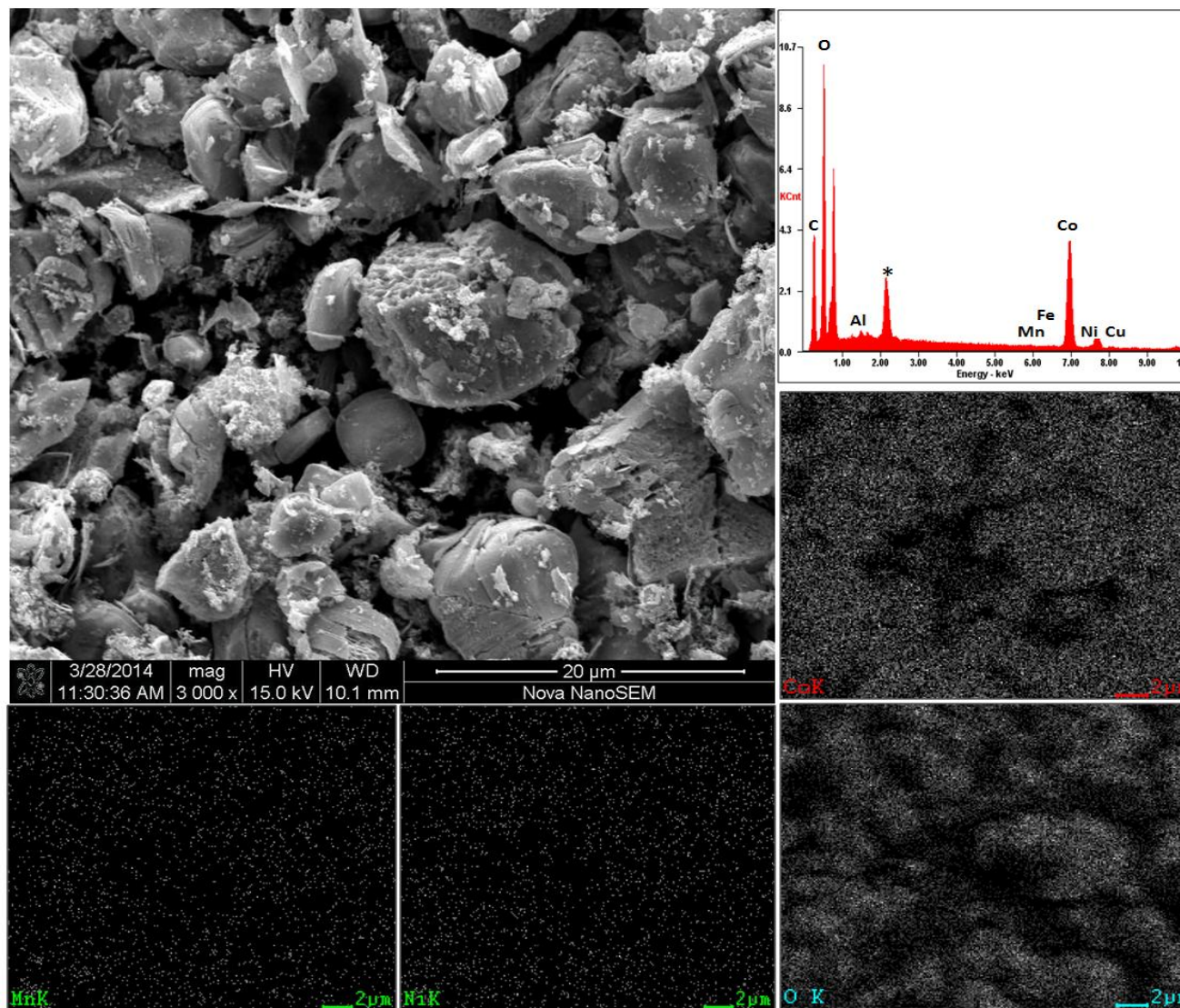
Fig. 2.4: SEM-EDAX analysis with mapping of constituent elements* in cathode material of spent LIBs
(* for coated gold; Li distribution not reflected in SEM)

2.2.1 Dismantling of spent NiMH batteries and characterization of electrode powder

To obtain the battery material for leaching, the components of Ni-MH batteries were subjected to physical separation by crushing. The batteries consist of steel case, battery electrode as well as nylon separator and each material has different characteristics such as particle size and specific gravity. The batteries were agitated and crushed by scutter crusher in the water medium. Heavy particles mainly the steel case settled down and the nylon separator being lighter floated out, leaving the electrode material dispersed in the water. After scrubbing, floating material was first removed from the water. The suspended fraction containing black powder of the electrode was separated by wet screening using a sieve of 20 µm size. Heavy materials settled in the bottom layer, were also separated by the same method. After separation, the electrode powder was collected, dried at 353 K for 24 h, and was characterized for its particle size, chemical analysis, phase identification by XRD (Bruker™ D8 Discover) and morphological features by SEM attached with EDAX system after gold coating (FEI-Quanta™). The particle size of the electrode powder was determined by a laser particle size analyzer (Malvern®, UK) as in the previous section. The average particle size of the electrode material was found to be 26.06 µm (Fig. 2.5) with the specific surface area of 1.6195 m^2/g. The electrode powder of the spent batteries (Table 2.3) contains ~ 59% Ni, 4.6% Co and 18.3% of rare earth metals along with other metals including the manganese and zinc. Among the rare earth metals, the maximum is samarium (6.2%) followed by neodymium (4.5%), lanthanum (2.7%), cerium (2.58%) and praseodymium (2.29%).

Table 2.3: Chemical composition of spent Ni-MH battery powder

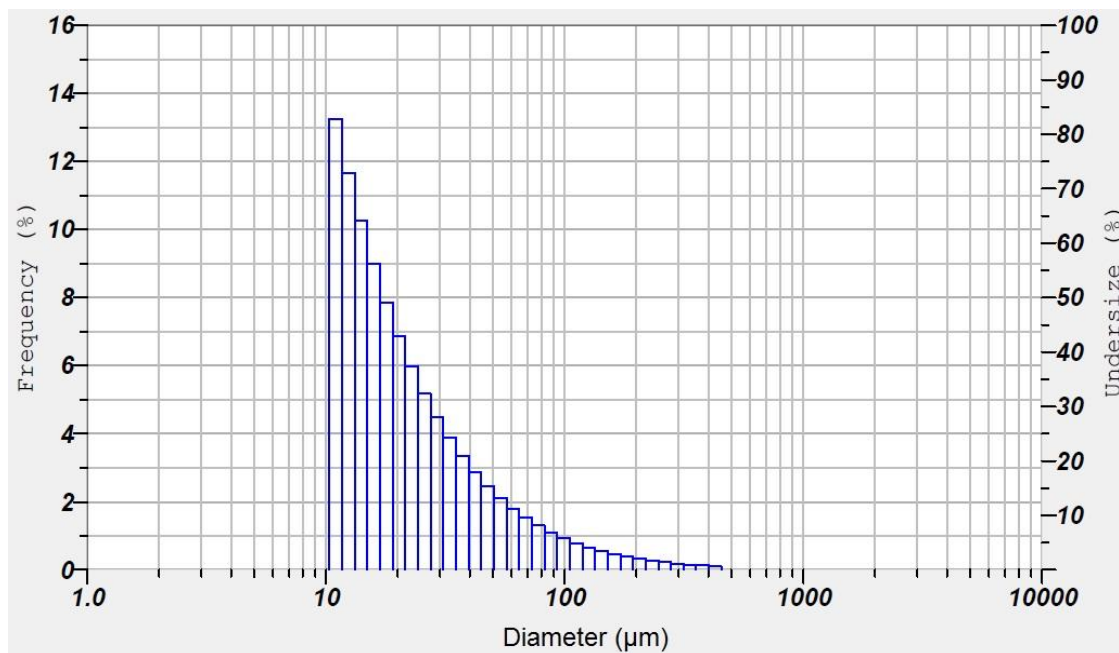| Element	Ni	Co	Mn	Fe	Zn	La	Nd	Sm	Pr	Ce
Wt. %	58.9	4.6	2.9	2.8	2.0	2.7	4.5	6.2	2.29	2.58

Fig. 2.5. Relative frequency distribution of NiMH battery electrode powder vs diameter (in μm) for particle size analysis

2.2.2 XRD analysis of electrode material of spent NiMH batteries

The XRD pattern of the electrode powder is shown in Fig. 2.6. The XRD analysis (Table 2.4) clearly shows the presence of $Ni(OH)_2$, Ni, Nd_2Ni_7, Ni_5La and Co_2NiO_4 as the major phases, whereas $CeCo_3$, Sm_2Fe_{17}, Ce_2Ni_7, $NiMn_2O_4$, (Ni, Zn) Fe_2O_4 being the minor phases. The SEM image of the powder sample (Fig. 2.7) shows the presence of dispersed metal aggregates with strong intercalation of the nickel based phases as identified by the XRD analysis.

SEM image of the electrode powder recorded at somewhat higher magnification (Fig. 2.8) also reflects the dispersed metal aggregates with further intercalation of the nickel containing phases; the corresponding EDAX is depicted below the micrograph (left side). The elemental mapping (Fig. 2.8) shows the distribution of the constituent elements all around the micrograph, which also exhibits the presence of high amount of nickel along with some cobalt and other base metals. The scarce spots in the SEM images mapped for manganese, zinc and iron reflect the low concentrations of these

metals that are scattered in the material. The distribution of the rare earth metals is however, not presented in the elemental mapping.

Table 2.4: XRD analysis of NiMH battery material before processing

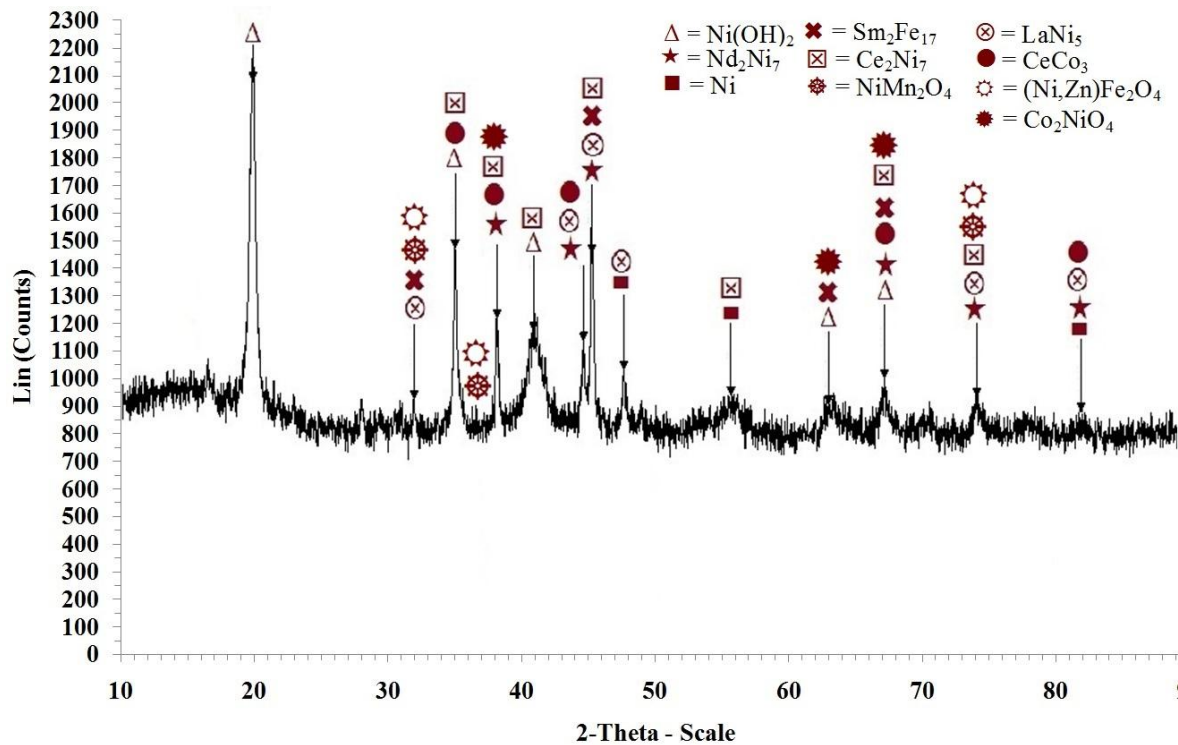| Sample	Major phases		Minor Phases	
	Phases	*JCPDS file No.*	*Phases*	*JCPDS file No.*
Electrode material	$Ni(OH)_2$	011047	$CeCO_3$	200263
	$LaNi_5$	421191, 170126	Sm_2Fe_{17}	481789
	Nd_2Ni_7	221174	Ce_2Ni_7	260042
	Ni	011260	$NiMn_2O_4$	840542
	Co_2NiO_4	021074	$(Ni, Zn)Fe_2O_4$	080234

Fig. 2.6: XRD of the spent Ni-MH battery electrode powder
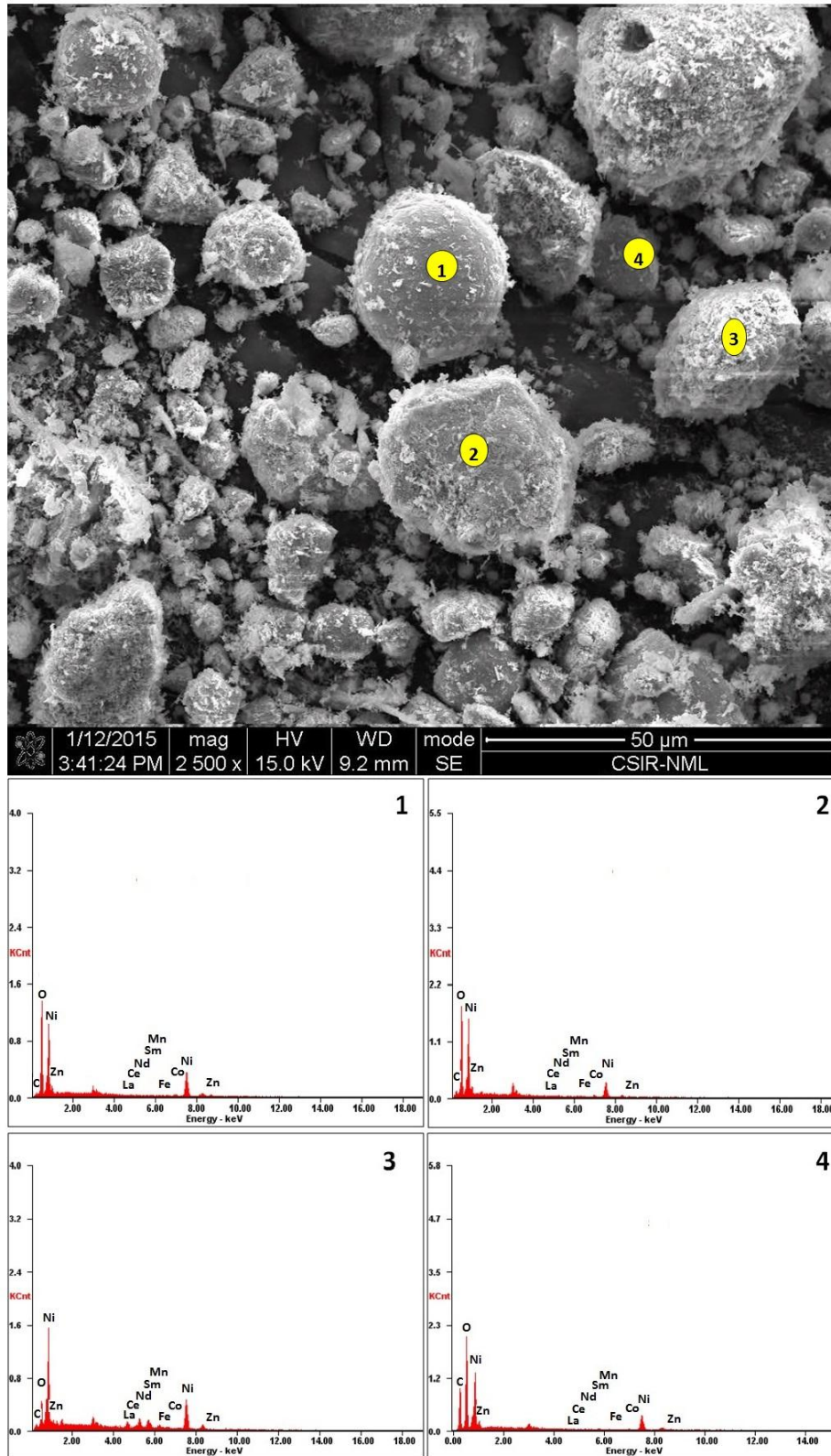
Fig. 2.7: SEM-EDAX of the spent NiMH battery electrode powder
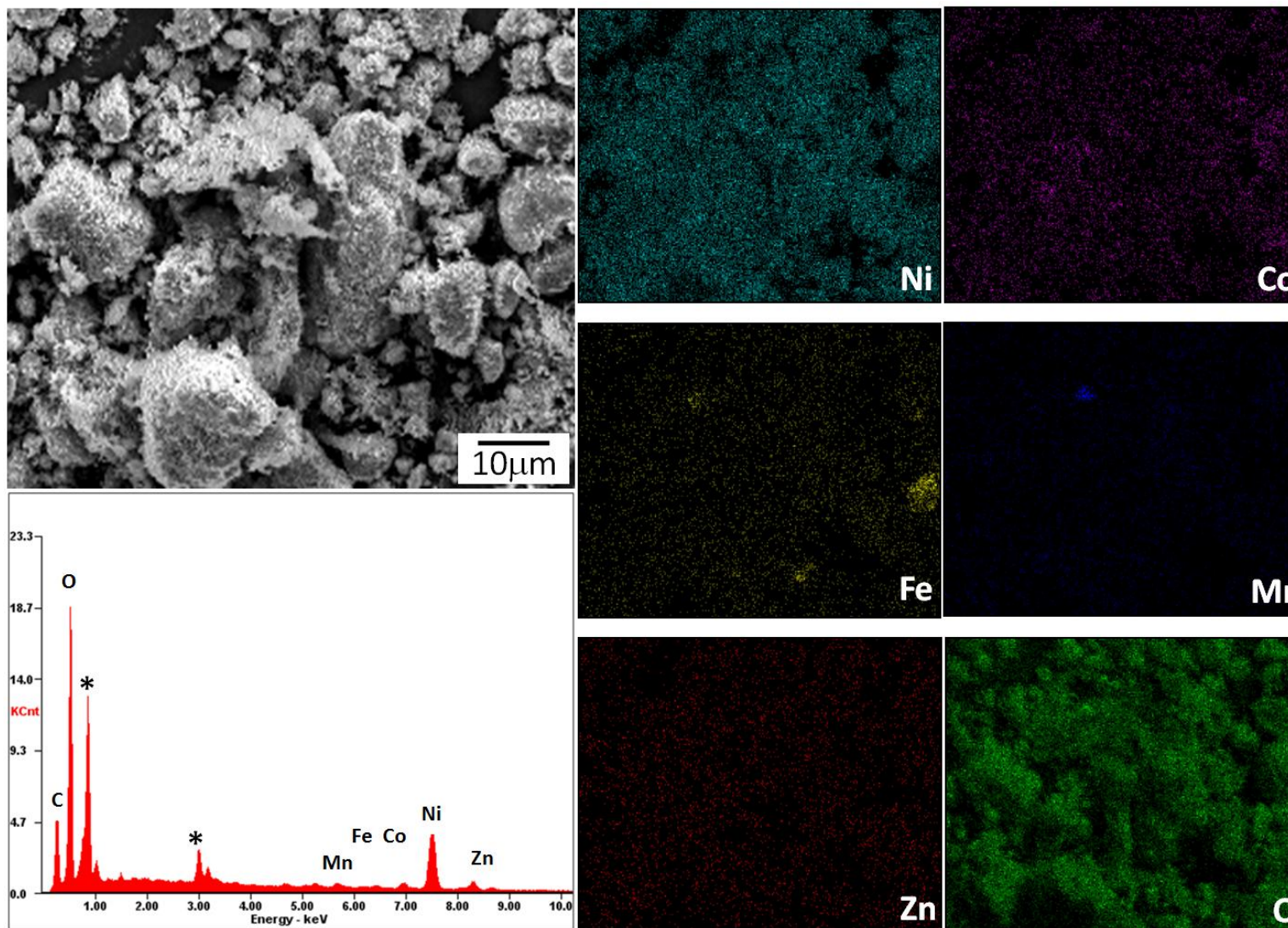
Fig. 2.8: SEM-EDAX analysis with mapping of the constituent elements in the spent Ni-MH battery material (* for gold coating)

2.3 Leaching of metals from the battery material

Considering the high metal yields and the economic prospects for the recovery of valuable metals in sulfuric acid, this was chosen as the lixiviant in most cases unless stated otherwise. Leaching study was carried out in a temperature controlled three necked flat bottom borosilicate glass reactor (cap. 500 mL) on hot-plate cum magnetic stirrer (IKA$^{®}$) at the desired rpm. A reflux condenser was fitted to the leaching vessel to avoid the loss due to evaporation. A known amount of the battery powder was transferred to the leach solution containing the desired concentration of the sulfuric acid maintained at a preset temperature. The slurry was stirred with a magnetic needle at 500 rpm unless specified otherwise for the entire duration of the leaching. In order to examine the progress of leaching, samples were withdrawn at different time intervals and were analyzed for the metals of interest after filtration. The redox potential during the leaching was also measured in a few cases wherever it was considered necessary, using a pH meter (Toshniwal, India, CL 46+) against a saturated calomel electrode (SCE); the redox potential values presented in the thesis are shown as E_{SCE}. At the end of the leaching, the slurry was filtered over a Büchner funnel using Whatman filter paper (42 No), the residue was washed with distilled water and dried overnight at 353 K in an electric oven. The leaching efficiency was calculated by analyzing the metals in the filtrate after necessary dilution and acidification. In a few cases residues were also analyzed after digesting in the aqua-regia and adding additional acid (HCl). Satisfactory mass balance was obtained in such set of experiments.

All the solutions generated in the leaching were analyzed by AAS (Atomic Absorption Spectrometer) and ICP-OES. Residue samples after drying were characterized by chemical analysis, SEM /EDAX and XRD analysis. The leach liquor obtained under the optimum conditions was subjected to precipitation studies to recover the leached metals using a suitable agent. Each experiment was performed two times, and the average of two replicates was considered for computing the final metal recovery.

2.3.1 Recovery of metals from the leach liquors by precipitation

Precipitation study was carried out in a temperature controlled three necked flat bottom borosilicate glass reactor (cap. 500 mL) on hot-plate cum magnetic stirrer (IKA®). In order to recover the metals, the leach liquor obtained as above was subjected to precipitation by using oxalic acid, NaOH or Na_2CO_3. Thus a known amount of leach liquor was taken in the flask and the precipitation agent was added through a burette attached to the neck of the vessel with occasional mixing. The pH of the solution was continuously measured using the pH meter attached to the flask. After the desired pH was attained the agitation was provided for a known period of time and the final precipitate was filtered over a Büchner funnel using Whatman filter paper (42 No) yielding the respective metal salt. The precipitated material was washed with distilled water, dried at 353 K in an electric oven for overnight and was stored in a desiccator.

The precipitation efficiency of the metal was calculated by analyzing the metals in the filtrate after necessary dilution. Satisfactory mass balance was obtained for each set of the experiment. The precipitated material was also characterized for phase identification by XRD analysis and morphology and elemental analysis by SEM-EDAX studies.

All the chemicals used in the experiments were of analytical grade reagents.

2.4 Process intensification by baking of the battery powder

As a part of process intensification, the battery materials obtained from the two types of spent batteries were baked in H_2SO_4 to examine its effect on the leach recovery of various metals. The baking experiments were carried out in a temperature controlled electrically operated muffle furnace (Model- Naskar and Co.™, India). In each experiment, a known weight of cathode active material of spent LIBs/ electrode powder of NiMH battery was thoroughly mixed with a suitable amount of concentrated sulfuric acid (98%) in a porcelain crucible (boat type). The crucible was weighed and transferred to the muffle furnace, which was preheated to the desired temperature. After a certain time, the crucible was taken out of the furnace, cooled to room temperature and weighed. The baked material being quite friable was removed

from the crucible and was ground using a mortar-pestle. Various baking parameters such as baking temperature and time, and acid concentration were optimized for maximum solubility of the metallic values. The material was initially characterized by XRD analysis to determine the phase changes as a result of acid baking.

 The acid baked powder was subjected to neutral leaching in water (leach-I) to determine the solubility of the metals under a set of conditions including time, temperature and pulp density using the same experimental set up as described in previous section (2.3). The water leached sample may be suitably characterized for chemical composition, phase identification and morphological features. In view of the fact that the electrode phases will undergo transformation because of the acid baking, dissolution of all the metals may not follow the same trend as that observed during the acid leaching itself and all metals may not dissolve completely in the leach-I stage. Therefore, it might be useful to investigate the re-leaching of the metals from the residue sample (leach-II) after the neutral leach with the aim of recovering as much as possible the residual metals using an acid. Along with the optimization of the leaching parameters to achieve the best overall leaching efficiency, it would also be interesting to correlate the metal dissolution at every stage of the processing with the characterization studies by XRD and SEM-EDAX.